

Unsteady Open-Channel Flow

- Its mean structure and suspended load transport -

By TU H.* , W. H. GRAF** and N. TAMAI***

Reported here are the unsteady flow investigations carried out by the authors in recent years. These include mainly four parts: 1) longitudinal component of the point velocity, which was carefully measured in hydrographs simulated in a tilting flume; 2) friction velocity and flow resistance, the results of which can be used to understand field data; 3) shear stress on horizontal planes and its vertical distribution, of which the characteristics are theoretically explained; and 4) suspended-load transport. Also presented is a theoretically derived dimensionless parameter of flow unsteadiness. Major results are summarized in Table 2.

Keywords: *unsteady flow, velocity profile, friction, shear-stress profile, suspended-load transport*

1 Introduction

Until recently, experimental study on unsteady flow in open channels, unlike that of steady flow, has been rare. Unsteady flow research, except for numerical modeling, has been mainly subjects of fluid mechanics. In the following we shall first try to distinguish different unsteady flow phenomena, and give a brief review of the existing unsteady-flow investigations, including laboratory and field studies.

There are different types of unsteady flows. Basically two forms of unsteadiness are involved (Telionis 1981): the erratic unsteady motion due to hydrodynamic instability and the organized motion due to the external disturbances. While the first is beyond the present discussion, the second may be subdivided into two categories: free surface flow; and non-free surface flow, such as unsteady flow in pipes and in wind tunnels. Free surface unsteady flow includes oscillatory flow encountered in coastal engineering and open-channel flow appeared in river engineering. Oscillatory flow experiments, though many (see for example, Knight 1978, Carr 1983), have been limited in either wind and water tunnels, or pipes, but rarely conducted in open channels.

Systematical experiments have been carried out to study unsteady open-channel flow, to the authors' knowledge, at the University of Canterbury, New Zealand, at the EPFL, Switzerland, and recently at Kyoto University. Phillips and Sutherland (1984) investigated spatial and temporal lag effect in bedload transport. Suszka (1987) conducted systematical experiments of bedload transport in unsteady flows. Song et al. (1991) investigated the turbulence characteristics in unsteady open-channel flow using both an acoustic Doppler Velocity Profiler and a hot-film anemometer. With a LDA system Nakagawa et al. (1993) measured the turbulent structures in unsteady channel flows.

Nouh (1989) examined unsteady flow effect on the armoring layer in a straight open channel. Flume experiments were also conducted to investigate alternate-bars in unsteady flow (Tubino 1989). Kuhnle (1992) studied bed-load transport in natural unsteady flows.

On the other hand, the flow resistance in unsteady open-channel flows is usually represented by the Manning's coefficient, n . In practice, the Manning n is firstly estimated from past experience, then calibrated against available field data (Fread 1989, Lebossé 1989). However, there exists rarely any investigation on the friction velocity in unsteady flows.

| | | | | |
|------------|----------|-------------|--------------------|-------------------|
| * Member | Dr. Eng. | Res. Assoc. | Dept. Civil Engrg. | Univ. of Tokyo |
| * | Ph.D | Professor | LRH, | EPFL, Switzerland |
| *** Member | Dr. Eng. | Professor | Dept. Civil Engrg. | Univ. of Tokyo |

2 Experiments

The experiments were conducted in a tilting flume (Tu 1991). It is 16.8m long, 0.6m wide and 0.8m high, with glass side walls and a smooth steel floor that was covered with gravels. The flume's bottom slope can be varied from -1% up to 9.7%. The pump was operated automatically by a computer.

Three capacity limnimeters were employed for measuring the water depths at three cross sections. The limnimeter has an accuracy of $\pm 1\%$. To measure the point velocities in unsteady flow, several micropropellers (manufactured by Nixon Instruments Ltd., UK) were used. The probes employed have a precision of 1% within the range of the measurements.

Before we set to generate hydrographs in the laboratory flume, those in natural rivers (in different countries) were examined (Tu 1991). It was shown that: 1) a natural hydrograph usually takes a skewed shape, with the water depth first increasing somewhat faster in the rising branch before decreasing relatively slowly in the falling branch; 2) the water depth reaches its maximum value D_{\max} at about $t_p = 1/3\Delta T$, where t_p is the time instant corresponding to D_{\max} , and ΔT is the total time duration of the hydrograph (Fig.1); 3) $\Delta D / \Delta T_r = 10^{-4} \sim 10^{-3}$ (m/s).

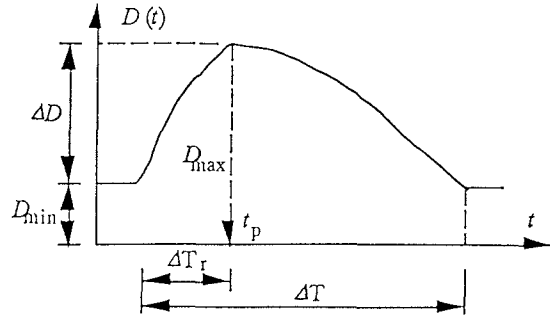


Fig.1 Typical Shape of A Natural Hydrograph

Table 1 Data range of the hydrographs investigated

| Hydro-graph No. | S_0 | d_s (cm) | ΔT (s) | ΔT_r (s) | D (cm) (min.,max.) | V (cm/s) (min.,max.) | $F_r = V / \sqrt{gD}$ (min.,max.) |
|-----------------|-------|---------------|-------------------|---------------------|-------------------------|---------------------------|--------------------------------------|
| NS1(1) | 0.002 | 1.35 | 110 | 36 | (9.0, 21.2) | (40.8, 94.9) | (0.43, 0.66) |
| NS1(2) | 0.002 | 1.35 | 110 | 38 | (9.3, 22.0) | (36.3, 93.4) | (0.38, 0.64) |
| NS1(3) | 0.002 | 1.35 | 110 | 38 | (9.9, 22.5) | (39.7, 97.7) | (0.40, 0.66) |
| NS2(1) | 0.002 | 1.35 | 220 | 76 | (6.6, 21.6) | (30.7, 96.1) | (0.38, 0.67) |
| NS2(2) | 0.002 | 1.35 | 220 | 68 | (7.0, 22.5) | (28.4, 95.7) | (0.34, 0.65) |
| NS2(3) | 0.002 | 1.35 | 220 | 80 | (7.2, 23.2) | (29.1, 95.9) | (0.34, 0.64) |
| NS3(1) | 0.002 | 2.30 | 110 | 46 | (14.2, 24.7) | (68.3, 122.9) | (0.58, 0.81) |
| NS3(2) | 0.002 | 2.30 | 110 | 46 | (15.4, 27.0) | (61.8, 120.0) | (0.50, 0.75) |
| NS3(3) | 0.002 | 2.30 | 110 | 46 | (15.7, 27.0) | (60.5, 121.5) | (0.48, 0.76) |
| NS4(1) | 0.002 | 2.30 | 220 | 72 | (11.5, 24.9) | (58.7, 123.7) | (0.55, 0.81) |
| NS4(3) | 0.002 | 2.30 | 220 | 74 | (12.9, 27.2) | (49.1, 115.6) | (0.44, 0.73) |
| NS5(1) | 0.005 | 2.30 | 110 | 52 | (13.0, 23.6) | (76.0, 130.9) | (0.68, 0.87) |
| NS5(3) | 0.005 | 2.30 | 110 | 48 | (13.8, 25.5) | (68.4, 129.4) | (0.59, 0.83) |

Bearing in mind the characteristics of the natural hydrographs mentioned above, 13 hydrographs were passed in the laboratory flume. The parameters showing the hydrographs' characteristics are given in Table 1, where S_0 is the flume's bottom slope, d_s the gravel diameter, V the depth-averaged velocity, F_r the Froude number. The other symbols are referred to in Fig.1.

Ideally, the velocity measurement at a point should be carried out by repeating as many times as possible the same hydrograph. However, due to the limited storage capacity of the data-acquisition system and the time-consuming process, many repeated measurements at a point were impossible. On the other hand, with a sampling frequency of 20Hz, it was seen that repeating more than five times did not improve significantly the precision for determining the time-mean point velocity (this was found in a pre-study, when the measurements at one point was repeated one hundred times). So it was decided to repeat the measurement 5 times at each point. The short-time-average method (Bendat and Piersol 1986) was used to calculate the time-mean point velocity.

3 Unsteadiness parameter

It is argued that there should be a dimensionless parameter which indicates the flow unsteadiness. This parameter can be derived theoretically (Tu 1991), as:

$$\beta = K \left(-\frac{D}{V} \frac{dV}{dt} \right) \quad (1)$$

where the coefficient K depends on the relative roughness and the velocity distribution (Tu and Graf 1992a). For negative β -values, the flow is an accelerating one and for positive β -values, the flow is a decelerating one.

The calculation of the unsteadiness parameter, β , using Eq.1, allows comparison of the measured velocity profiles in unsteady open-channel flow with those from other types of flow. And as we shall see in the following, it plays an important role in studying unsteady open-channel flows.

4 Velocity profiles

4.1 Point-velocity variation with time and water height

Time variations of point velocities, $u(y, t)$, at different levels within the entire water depth are shown in a figure inserted in Table 2 (note that for each hydrograph the measurements were performed at 23 to 26 different levels). It can be observed that throughout the water column, the point velocities near the water surface arrive at their maximum values earlier than those near the bottom. This is due to the fact that the relative importance of inertia over viscosity forces gets greater as one moves away from the bed. With the point velocities one can now obtain the velocity profile at any time instant.

4.2 Velocity profiles in the rising and falling branch; for equal water depth

The velocity profiles in the rising and falling branch, $u(y)$, for equal water depth, are also shown in a figure inserted in Table 2. It is seen that:

- 1) at the same water height, y , here given as y/D , the point velocity, u , in the rising branch is generally larger than the one in the falling branch;
- 2) this difference of the point velocities, u , between the rising and the falling branch gets larger on approaching the water surface;

Similar observations are reported by Suszka (1987) and Grishanin (1979).

4.3 Analysis

It was found that the velocity profiles follow the Coles law (Tu and Graf 1992a):

$$\frac{u}{u_*} = \frac{1}{\kappa} \ln \frac{y}{d_s} + B_r + \frac{2\Pi}{\kappa} \sin^2\left(\frac{\pi}{2} \frac{y}{D'}\right) \quad (2)$$

where: D' is the water height where the maximum point velocity in a velocity profile, u_{\max} , is measured; κ , the Karman constant; B_r , a numerical constant of integration; Π , the Coles parameter expressing the wake strength; and $u_* = u_{*sv}$, the friction velocity in unsteady flow (see next section).

The experimental data show that, while the B_r -values vary in the range of $3.8 < B_r < 14.5$ with the relative roughness in the range of $0.058 < d_s/D < 0.16$, the B_r -value may be represented by a constant, being $B_r = 8.5$. The present data set (273 velocity profiles in all, with the β -value varying from -0.23 to 0.15) renders for the B_r -values an empirical relation:

$$B_r = 8.1 \beta + 8.1 \quad (3)$$

It was also shown (Tu and Graf 1992a) that the B_r -values show an increasing tendency during the passage of the hydrographs, being lower in the rising branch (accelerating flow) and usually higher in the falling branch (decelerating flow) of each hydrograph.

For the Π -value in Eq.2, the present data set produces an empirical relation, such as:

$$\Pi = 1.02 \beta + 0.46 \quad (4)$$

Plotted versus β , the Π -values from the present data set compared rather well with those reported in the literature, for different types of flows. This indirectly confirms that β is indeed an important parameter.

It was also found that Π becomes more pronounced in the falling branch (decelerating flow) compared with the one in the rising branch (accelerating flow).

5 Friction velocity

The friction velocity in the present study (labeled as u_{*sv} in the following) was determined using the full St. Venant equation, as (Tu and Graf 1993):

$$u_{*sv} = \sqrt{gD[S_0 + \frac{1}{C} \frac{\partial D}{\partial t} - \frac{1}{g} \frac{\partial V}{\partial t} (1 - \frac{V}{C})]} \quad (5)$$

Assuming that the hydrographs investigated are kinematic or non-subsiding monoclinal waves, the wave velocity, C , can be determined as (Tu 1991):

$$C = V + D \frac{\partial V}{\partial t} / \frac{\partial D}{\partial t} \quad (6)$$

For the present study, the friction velocity, u_{*sv} (in Eq.5), can be calculated from the time-records of the depth-averaged velocity, $V(x,t)$, and of the water depth, $D(x,t)$. An example of the obtained results is given in Table 2. Also shown is the *apparent* friction velocity, $u_{*s} = \sqrt{gDS_0}$, calculated by assuming that the friction slope equals the bottom slope. The ratio of the *true* value of the friction velocity, u_{*sv} , given with Eq.5, to its *apparent* value, u_{*s} , is:

$$\frac{u_{*sv}}{u_{*s}} = \sqrt{1 + \frac{3}{5S_0} \frac{\partial D}{\partial t} (1 - \frac{4}{9} F_r^2)} \quad (7)$$

From the calculated friction velocity and the measured depth-averaged velocity, it is possible to obtain the friction coefficient, f , defined as $f = 8(u_{*sv}/V)^2$, an example of which is shown in Table 2. The variations of the friction coefficient show similar tendency as observed by Coleman (1962) in natural flood events.

6 Shear-stress profiles

In unsteady open-channel flow the shear stress at a certain level can be derived as (Tu and Graf 1992b):

$$\tau(y,t) = \tau_1 + \tau_2 + \tau_3 = \rho g S_0 (D - y) + \rho g \frac{1}{C} \frac{\partial D}{\partial t} (D - y) - \rho \int_y^D \frac{\partial u}{\partial t} (1 - \frac{u}{C}) dy \quad (8)$$

In other words, the shear stress may be considered as being composed of three parts: τ_1 , the contribution from the bottom slope; τ_2 , the contribution from the time variation of the water depth; and τ_3 , the contribution from the time variation of the point velocity. At a certain time instant, both τ_1 and τ_2 vary linearly with the water height, y . However, since the time derivative, $\partial u / \partial t$, varies with not only time but also the water height (see the corresponding figure in Table 2), the contribution τ_3 , and consequently the total shear, $\tau(y,t)$, varies non-linearly with the water height.

6.1 Shear-stress, $\tau(y,t)$, variations with time and water height

As can be seen from the figure in Table 2, the shear stress near the water surface arrives at its maximum value *later* than the one near the bottom. Similar results are reported by Hayashi and Ohashi (1981, Fig.9) from their direct shear-stress measurements with a hot-film probe in water-tunnel oscillatory flows.

6.2 Shear-stress distributions in the rising and falling branch; for equal water depth

The shear-stress profiles in the rising and falling branch, for equal water depth, are also shown in Table 2. It can be observed that:

- 1) at the same water height, y , here given as y/D , the total shear stress in the rising branch can be considerably larger than the one in the falling branch. This was also observed by Hayashi et al. (1988);
- 2) the difference of the shear stress between the rising and falling branch gets larger near the bottom;
- 4) the shear-stress profiles are non-linear.

It is seen, and can be explained theoretically (Tu and Graf 1992b), that the shear-stress profiles are concave in the rising branch when the flow is accelerating ($\beta < 0$), but are convex in the falling branch while the flow is decelerating ($\beta > 0$). Similar results have been reported by Bradshaw (1967) and Herring and Norbury (1967) for steady, non-uniform turbulent boundary-layer flow, by Grishanin (1979, p.64) for steady, non-uniform open-channel flow and by Justesen (1988, p.96) for oscillatory flow.

7 Suspended-load transport

To deal with suspended-load transport problems in natural rivers, sometimes it is enough to know the cross-sectional mean concentration, at other times a knowledge of the vertical concentration profile is necessary, requiring thus one-dimensional or two-dimensional treatments, respectively.

7.1 One-dimensional treatment

In the case where non-equilibrium sediment transport occurs, the mobile bed level will undergo changes (Fig.2), either due to aggradation ($\partial d / \partial t > 0$) or due to degradation ($\partial d / \partial t < 0$). The sediment concentration in non-equilibrium transport can be derived as (Tamai and Tu 1992):

$$C_{us} = C_s - \int_{x_1}^{x_2} \left\{ \alpha_1 \frac{1}{V} \frac{\partial D}{\partial t} + \alpha_2 \frac{1}{g} \frac{\partial U}{\partial t} - \alpha_3 \frac{\partial d}{\partial t} \right\} dx \quad (9)$$

in which all the three coefficients:

$$\alpha_1 = \frac{6\gamma_m}{5g(\gamma_s - \gamma)D^2 S_0} \left(1 - \frac{4}{9} F_t^2\right) ; \quad \alpha_2 = \frac{2\gamma_m}{(\gamma_s - \gamma)D} \quad \text{and} \quad \alpha_3 = \frac{\{m\gamma_s + (1-m)\gamma\}}{g\gamma_m} \frac{V}{D}$$

are positive. In the above equations: C_{us} is the cross-sectional mean concentration in unsteady flow; C_s , the cross-sectional mean concentration in an equivalent steady flow; m , the percentage of the sediments existing in the mobile layer; U , the cross-sectional mean velocity; x , the longitudinal coordinate; d , the thickness of the mobile layer; and γ_m is the unit weight of the sediment-water mixture.

In natural flood events, it is usually observed that the maximum cross-sectional mean velocity arrives ahead of the maximum water depth (Tu 1991). Bearing this on mind and seeing that degradation ($\partial d / \partial t < 0$) occurs most probably in the rising branch, while aggradation ($\partial d / \partial t > 0$) usually appears in the falling branch, one may conclude from Eq.9 that the maximum cross-sectional mean velocity arrives ahead of the maximum sediment concentration, which in turn is followed by the maximum water depth. This point is evidenced by a set of field data collected in Hokkaido's Ishikari River (see Tamai and Tu 1992).

Also to be noted is that, for an equal water depth the suspended-load concentration in the rising branch is larger than the one in the falling branch; on the contrary, for an equal depth-averaged velocity the suspended-load concentration in the rising branch is smaller than the one in the falling branch, as can be observed from Fig.3.

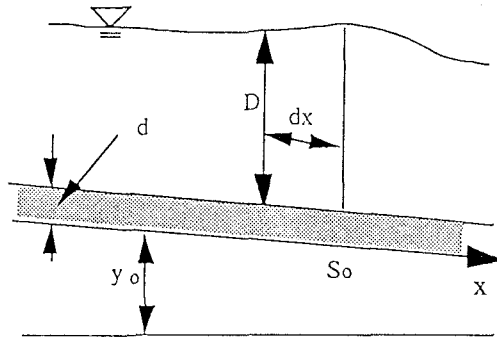
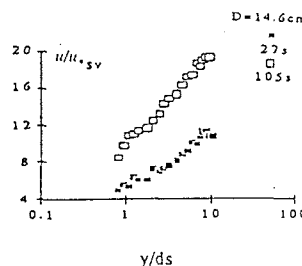
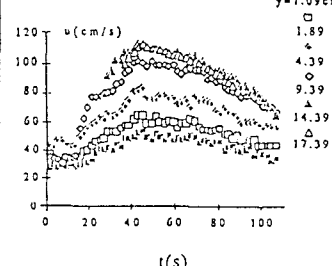
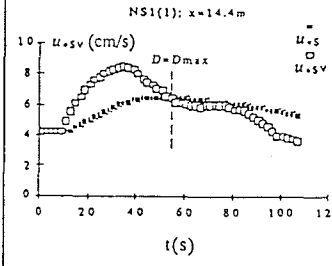


Fig.2 A Definition Sketch

Table 2 Mean Structure in

| Unsteadiness Parameter; | | |
|-------------------------|--|---|
| Item | Point velocity | Fric- |
| | $u(y)$ | $u^*(t)$ |
| Form | $\frac{u}{u_*} = \frac{1}{\kappa} \ln \frac{y}{d_s} + B_r + \frac{2H}{\kappa} \sin^2(\frac{\pi}{2} \frac{y}{D});$ $B_r \sim 8.5, \Pi = 0.0 - 1.0$ | $u_{*sv} = \sqrt{gD \{S_0 + \frac{1}{C} \frac{\partial D}{\partial t} [1 - \frac{(C-V)^2}{gD}]\}}$ |
| Fig. | NS1(1), D=20.5cm  | NS1(1)   |

7.2 Two-dimensional treatment

Assuming a constant sediment-diffusion coefficient, Tu et al. (1993) presented an analytical study on the suspended-load variations with time and height in unsteady open-channel flows. A notable feature in their work was the introduction of the concept of *sediment-wave celerity*.

As is mentioned above, the hydrographs investigated are kinematic waves. The suspended-load concentration measured at a certain station during a flood event can be expressed in the form of a histogram, as can be the flow discharge. From the histograms observed in natural rivers, it might be reasoned that the suspended load also participate (as does the flow discharge), with a certain speed - here designated as *sediment wave celerity* - in the kinematic wave motion.

The initial and boundary conditions are (Fig.4):

at $t = 0, c = f(y)$ for $0 < y < D$

$$\epsilon \frac{\partial c}{\partial y} \Big|_{y \rightarrow 0} = -\omega c_a \tag{10}$$
$$\epsilon \frac{\partial c}{\partial y} \Big|_{y = D} = -\omega c \Big|_{y = D}$$

where: c is the suspended-load concentration at a point in space; ω , the particle settling velocity; c_a , a reference concentration; $f(y)$, an arbitrary function of y ; and ϵ , the sediment-diffusion coefficient.

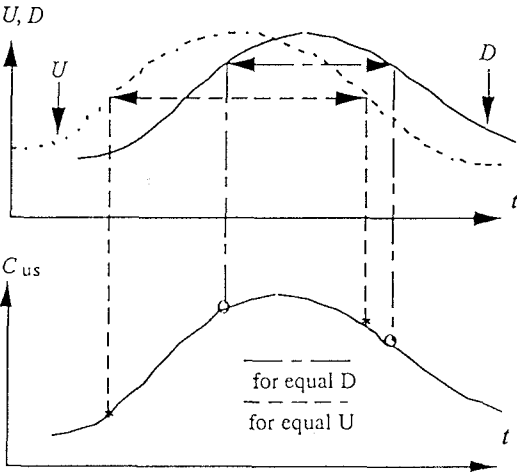


Fig.3 Sediment Concentration during a Hydrograph

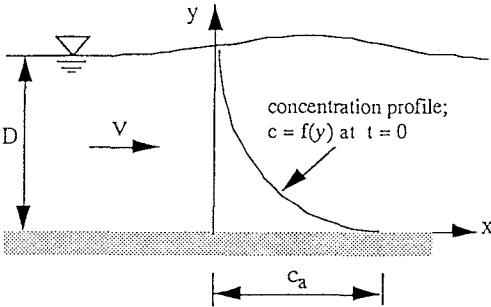


Fig.4 A Sketch of the Boundary Conditions

Unsteady Open-Channel Flow

| $\beta = K \left(-\frac{D}{V^2} \frac{dV}{dt} \right)$ | | | | |
|--|--|--|--------------|------------------|
| tion | | shear stresses | | concentration |
| $f(t)$ | | $\tau(y)$ | $\tau(y, t)$ | $c(t)$ $c(y, t)$ |
| $f = 8gD \left\{ S_0 + \frac{1}{C} \frac{\partial D}{\partial t} \left[1 - \frac{(C-V)^2}{gD} \right] \right\} / V^2$ | | $\tau(y, t) = \tau_1 + \tau_2 + \tau_3$ $= \rho g S_0 (D-y) + \rho g \frac{1}{C} \frac{\partial D}{\partial t} (D-y) - \rho \int_y^D \frac{\partial u}{\partial t} \left(1 - \frac{u}{C} \right) dy$ | | Eq.9 Eq.11 |
| | | | | — — |

Using the sediment-wave celerity concept and the boundary conditions (Eq.10), an analytical solution for the concentration at a point in space was derived from the diffusion equation, as (Tu et al. 1993):

$$c = c_a e^{-(W/E)y} + e^{-0.5(W/E)y} \sum_{n=1}^{\infty} e^{-(\alpha_n^2 E + 0.25 W^2/E)t} a_n \left(\cos \alpha_n y + \frac{W}{2E\alpha_n} \sin \alpha_n y \right) \quad (11)$$

with
$$a_n = \frac{2\alpha_n}{(\alpha_n^2 + \frac{W^2}{4E^2})D + \frac{W}{E}} \int_0^D \left\{ [f(y) - c_a e^{-(W/E)y}] e^{0.5(W/E)y} \left(\cos \alpha_n y + \frac{W}{2E\alpha_n} \sin \alpha_n y \right) \right\} dy$$

$$W = \omega / (1 - \frac{V}{C}), \quad E = \epsilon / (1 - \frac{V}{C}); \quad 2ctg\alpha D = (\alpha D) / (\frac{WD}{2E}) - (\frac{WD}{2E}) / (\alpha D)$$

Equation 11 is the solution for the suspended-load concentration in unsteady, two-dimensional open-channel flows. It gives the vertical profile of suspended-load concentration at any time instant. For example, if $f(y) = c_0$, then Eq.11 would predict the concentration after a sediment-water mixture with a known concentration is released into the flow. Further, if $c_0 = 0$, that would be a case of scouring, when in the beginning only water (clear of sediment) is supplied at the station under study. Another example would be for the rate of deposit under equilibrium condition to be zero ($c_a = 0$), simulating thus the case where appears settling out from equilibrium concentration to zero concentration at all water depths.

8 Conclusion

An investigation on the mean structure of unsteady open-channel flows is presented in this paper. *Velocity profiles* in hydrographs simulated in a flume were carefully measured. From the experimental results the *friction velocity* was determined using the full St. Venant equation. The findings on the *friction coefficient* could be used to understand a set of field data reported in the literature. The *shear stress* on horizontal planes and its vertical profiles are determined from the time records of the point velocities and that of the water depth, using the equation of motion. At a certain station, it is shown that the maximum mean velocity arrives ahead of the maximum sediment concentration and the maximum water depth, as was observed in a natural flood event. The variations of the suspended-load concentration with time and water height is investigated analytically.

9 References

- Bendat, J. S. and A. G. Piersol (1986), Random Data Analysis and Measurement Procedures, 2nd Edition, a Wiley-Interscience Publication, John Wiley & Sons, p.566.
- Bradshaw, P. (1967), The Turbulent Structure of Equilibrium Boundary Layers, J.Fluid Mech., Vol.29, part 4, pp.625-645.
- Carr, L.W., (1981), A Review of Unsteady Turbulent Boundary-Layer Experiments, in Unsteady Turbulent Shear Flows, IUTAM Symposium, Toulouse, France, Michel.R. et al. eds.
- Coleman, N. L. (1962), Observations of Resistance Coefficients in a Natural Channel, IASH, Commission of Land Erosion, Bari, Italy, October, pp.336-352.
- Fread, D. L. (1989), Flood Routing Models and the Manning n, in Channel Flow and Catchment Runoff, Intern. Confer. Cent. Manning's Formula and Kuichling's Rational Formula, Ed. B. C Yen.
- Grishanin, K (1979), Dynamika Ruslobich Potokob (Dynamics of Alluvial Flow), Hydrometeoizdat, Leningrad.
- Hayashi, T., M. Ohashi and M. Oshima (1988), Unsteadiness and Turbulent Structure of a Flood Wave, Proc. 20th Symp. on Turbulence, Japan Society of Fluid Mechanics.
- Herring H. and J. Norbury (1967), Some Experiments on Equilibrium Turbulent Boundary Layers in Favorable Pressure Gradient, J.Fluid Mech., Vol.27, pp.541-549.
- Justesen, P. (1988), Prediction of Turbulent Oscillatory Flow over Rough Beds, Coastal Engineering, No.12, pp.57-284.
- Knight, D. W. (1978), Review of Oscillatory Boundary Layer Flow, Proc. Am. Soc. Civ. Engrs, J. Hyd. Div., Vol.104, No.HY6, pp.839-855.
- Kunhle, R. A. (1992), Bed Load Transport during Rising and Falling Stages on Two Small Streams, Earth Surface Processes and Landforms, Vol.17, pp.191-197.
- Lebossé, A. (1989), Estimation of the Manning-Strickler Roughness Coefficient in Saint-Venant Equations, in Channel Flow and Catchment Runoff, Proc. Intern. Confer. Centennial of Manning's Formula and Kuichling's Rational Formula, Ed. Ben Chie Yen, pp.709-718.
- Nakagawa, H., I. Nezu, Y. Ishida, A. Kadota and H. Fujimoto (1993), Difference between Turbulent Structures in Unsteady Open-Channel Flows and Those in Pope Flows, Proc. of the Japanese Conf. on Hydr. Conf., JSCE, Vol.37, pp.373-378.
- Nouh, M. (1989), Self Armoring Process under Unsteady Flow Conditions, Proc. 23th IAHR Congress, Ottawa, Canada, pp.B49-B56.
- Phillips, B. C. and A. J. Sutherland (1984), Spatial and Temporal Lag Effects in Bedload Transport, Report 84/10, Dept. Civil Engineering, Univ. Canterbury, Rouse, H. (1937), Modern Conceptions of the Mechanics of Turbulence, Trans. Am. Soc. Civil Engrs., Vol.102.
- Song, T., W. Graf and U. Lemmin (1991), Turbulence Characteristics in Unsteady Open-Channel Flow, Annual Report, LRH-EPFL, Switzerland.
- Suszka, L. (1987), Sediment Transport at Steady and Unsteady Flow; A Laboratory Study, Doctoral dissertation No.704, Laboratoire de Recherches Hydrauliques, Ecole Polytechnique Fédérale, Lausanne, Switzerland.
- Tamai N. and Tu H. (1992), Sediment concentration in unsteady open-channel flow, Proc. 8th Congress of the Asian-Pacific Division, IAHR, Vol.-II, pp.1-10.
- Telionis, D. P. (1981), Unsteady Viscous Flows, Springer Series in Computational Physics, 408p.
- Tu H. (1991), Velocity Distribution in Unsteady Flow over Gravel Beds, Doctoral dissertation No.911, Laboratoire de Recherches Hydrauliques, Ecole Polytechnique Fédérale, Lausanne, Switzerland.
- Tu H. and W. H. Graf (1992a), Velocity distribution in unsteady open-channel flow over gravel beds, J. Hydrosience and Hydraulic Engineering, JSCE, Vol.10, No.1, pp.11-25.
- Tu H. and W. H. Graf (1992b), Vertical distribution of shear stress in unsteady open-channel flow, Proc. Instn Civ. Engrs Wat., Mart. & Energy, London, Vol.96, June, pp.63-69.
- Tu H. and W. H. Graf (1993), Friction in unsteady open-channel flow over gravel beds, J.Hydr. Res., Vol.31, No.1, pp.99-110.
- Tu H., N. Tamai and Y. Kawahara (1993), Suspended-Load Diffusion in Unsteady Open-Channel Flows, Proc. of the Japanese Conf. on Hydr. Conf., JSCE, Vol.37, pp.373-378.
- Tubino, M. (1989), Flume Experiments on Alternate-Bars in Unsteady Flow, Proc. International Workshop on Fluvial Hydraulics of Mountain Regions, Trent, Italy, pp.A93-A107.